

Fundamentals of half-metallic Full-Heusler alloys

K. Özdoğan*

Department of Physics, Gebze Institute of Technology, Gebze, TR-41400, Kocaeli, Turkey

E. Şaşıoğlu†

*Institut für Festkörperforschung, Forschungszentrum Jülich, D-52425 Jülich, Germany
and Fatih University, Physics Department, TR-34500, Büyükdere, İstanbul, Turkey*

I. Galanakis‡

Department of Materials Science, School of Natural Sciences, University of Patras, GR-26504 Patra, Greece

(Dated: October 22, 2018)

Intermetallic Heusler alloys are amongst the most attractive half-metallic systems due to the high Curie temperatures and the structural similarity to the binary semiconductors. In this review we present an overview of the basic electronic and magnetic properties of the half-metallic full-Heusler alloys like Co_2MnGe . Ab-initio results suggest that the electronic and magnetic properties in these compounds are intrinsically related to the appearance of the minority-spin gap. The total spin magnetic moment in the unit cell, M_t , scales linearly with the number of the valence electrons, Z_t , such that $M_t = Z_t - 24$ for the full-Heusler alloys opening the way to engineer new half-metallic alloys with the desired magnetic properties. Moreover we present analytical results on the disorder in $\text{Co}_2\text{Cr}(\text{Mn})\text{Al}(\text{Si})$ alloys, which is susceptible to destroy the perfect half-metallicity of the bulk compounds and thus degrade the performance of devices. Finally we discuss the appearance of the half-metallic ferrimagnetism due to the creation of $\text{Cr}(\text{Mn})$ antisites in these compounds and the Co-doping in $\text{Mn}_2\text{VAl}(\text{Si})$ alloys which leads to the fully-compensated half-metallic ferrimagnetism.

PACS numbers:

I. INTRODUCTION

Half-metallic ferromagnets, initially predicted by de Groot and his collaborators in 1983¹ using first-principles calculations are at the center of scientific research due to their potential applications. The minority-spin electrons in these compounds show a semiconducting electronic band-structure while the majority-spin electrons present the usual metallic behavior of ferromagnets. Thus such alloys would ideally exhibit a 100% spin polarization at the Fermi level and therefore they should have a fully spin-polarized current and should be ideal spin injectors into a semiconductor maximizing the efficiency of spintronic devices.²

Heusler alloys are well-know for several decades and the first Heusler compounds studied had the chemical formula X_2YZ , where X is a high valent transition or noble metal atom, Y a low-valent transition metal atom and Z a sp element, and crystallized in the $L2_1$ structure which consists of four fcc sublattices.^{3,4} Heusler compounds present a series of diverse magnetic phenomena like itinerant and localized magnetism, antiferromagnetism, helimagnetism, Pauli paramagnetism or heavy-fermionic behavior and thus they offer the possibility to study various phenomena in the same family of alloys.^{3,4} A second class of Heusler alloys have the chemical formula XYZ and they crystallize in the $C1_b$ structure which consists of three fcc sublattices; they are often called half- or semi-Heusler alloys in literature, while the $L2_1$ compounds are referred to as full Heusler alloys. The interest in these types of intermetallic alloys was revived after the prediction,¹

using first-principles calculations, of half-metallicity in NiMnSb , a semi-Heusler compound.

The high Curie temperatures^{3,4} exhibited by the half-metallic Heusler alloys are their main advantage with respect to other half-metallic systems (e.g. some oxides like CrO_2 and Fe_3O_4 and some manganites like $\text{La}_{0.7}\text{Sr}_{0.3}\text{MnO}_3$).⁵ While for the other compounds the Curie temperature is near the room temperature, for the half-metal NiMnSb it is 730 K and for the half-metallic Co_2MnSi it reaches the 985 K.³ A second advantage of Heusler alloys for realistic applications is their structural similarity to the zinc-blende structure, adopted by binary semiconductors widely used in industry (such as GaAs on ZnS). Semi-Heusler alloys have been already incorporated in several devices as spin-filters,⁶ tunnel junctions⁷ and GMR devices.⁸ Recently, also the half-metallic full-Heusler alloys have found applications. The group of Westerholt has incorporated Co_2MnGe in the case of spin-valves and multilayer structures⁹ and the group of Reiss managed to create magnetic tunnel junctions based on Co_2MnSi .^{10,11} A similar study by Sakuraba and collaborators resulted in the fabrication of magnetic tunnel junctions using Co_2MnSi as magnetic electrodes and AlO as the barrier and their results are consistent with the presence of half-metallicity for Co_2MnSi .¹² Moreover Dong and collaborators recently managed to inject spin-polarized current from Co_2MnGe into a semiconducting structure.¹³

In the present contribution we review our most recent results on the electronic properties of the half-metallic full-Heusler alloys obtained from first-principles electronic structure calculations. In section II we summa-

alize our older results on bulk compounds obtained using the full-potential version of the screened Korringa-Kohn Rostoker (KKR) method¹⁴ (see references 15,16,17 for an extended review). In the next sections we overview some of our results on the defects in the half-metallic full Heusler alloys obtained using the full-potential nonorthogonal local-orbital minimum-basis band structure scheme (FPLO)^{18,19} within the local density approximation (LDA)^{20,21,22} and employing the coherent potential approximation (CPA) to simulate the disorder in a random way.¹⁹ In section III we present the physics of defects in the ferromagnetic Heusler alloys containing Co and Mn like Co₂MnSi.^{23,24} The study of defect doping and disorder is of importance to accurately control the properties of half-metallic full-Heusler alloys.⁴ In section IV we demonstrate the creation of half-metallic ferrimagnets based on the creation of Cr and Mn antisites in Co₂(Cr or Mn)(Al or Si) alloys^{26,27} and we expand this study to cover the case of Co defects in ferromagnetic Mn₂VAl and Mn₂VSi alloys leading to full-compensated half-metallic ferrimagnets (also-known as half-metallic antiferromagnets).²⁸ Finally in section V we summarize and conclude.

II. ELECTRONIC AND GAP PROPERTIES – SLATER PAULING BEHAVIOR

The electronic, magnetic and gap properties of half-metallic full-Heusler compounds have been studied using first-principles calculations in reference 29. These results have been extensively also reviewed in reference 15, in the introductory chapter of 16 and in a chapter in reference 17. The reader is directed to them for an extended discussion. In this section we will only briefly overview these properties.

The electronic and magnetic properties of the full-Heusler compounds are similar to the half-Heusler compounds³⁰ with the additional complication of the presence of 2 Co atoms per unit cell as in Co₂MnGe. In the case of the semi-Heusler alloys there are exactly nine occupied minority-spin electronic states; one of s character and three of p-character provided by the sp atom and five bonding d-states originating from the hybridization between the transition metal atoms. In addition to these bands, in the case of full-Heusler alloys there are five states exclusively located at the Co sites and near the Fermi level and the Fermi level is located among these states so that three out of five are occupied and two of them unoccupied leading to small energy gaps.²⁹ Now there are 12 minority-spin occupied states and the compounds with 24 valence electrons like Fe₂VSb are semiconductors. If vanadium is substituted by a higher-valent atom, spontaneous spin polarization occurs, and the exchange splitting shifts the majority states to lower energies. The extra electrons fill in only majority states and the total spin moment per unit cell in μ_B , M_t , which is the number of uncompensated spins is the total num-

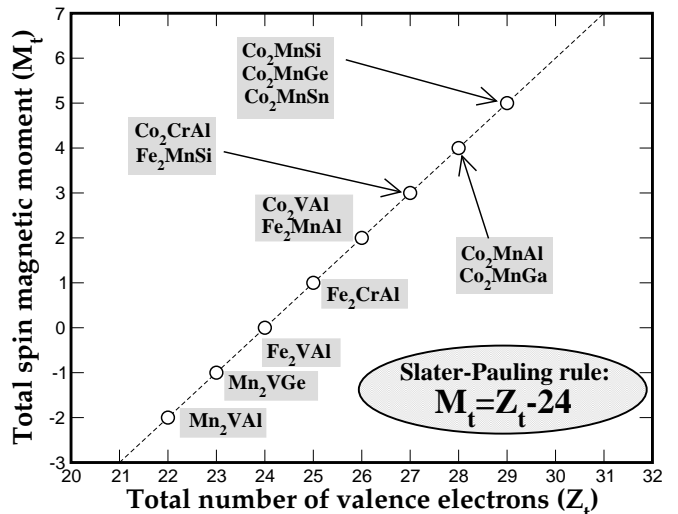


FIG. 1: Calculated total spin moment per unit cell in μ_B as a function of the total number Z_t of valence electrons per unit cell for the full Heusler alloys. The dashed line represents the Slater-Pauling behavior.

ber of valence electrons, Z_t , minus two times the 12: $M_t = Z_t - 24$. This behavior is the so-called Slater-Pauling behavior and e.g. half-metallic Co₂CrAl (27 valence electrons) has a total spin moment of $3 \mu_B$ and half-metallic Co₂MnSi (29 valence electrons) a spin moment of $5 \mu_B$. This rule provides a direct connection between the half-metallicity and the total spin moment which can be easily determined experimentally. In figure 1 we have plotted the calculated total spin moments for several full-Heusler compounds as a function of the total number of valence electrons. The dashed line represents the Slater-Pauling rule of half-metallic full Heusler alloys. Since 7 majority bands ($2 \times \text{Co } e_u$, $5 \times \text{Mn } d$) are unoccupied, the largest possible moment is $7 \mu_B$ and would occur if all majority d -states were occupied. Of course it would be impossible to get a compound with a total spin moment of $7 \mu_B$ but even $M_t = 6 \mu_B$ is difficult to obtain. As it was shown by Wurmehl et al.³¹, the on-site correlations in Co₂FeSi play a critical role for this compound and calculations within the LDA+U scheme, rather than the LDA, give a spin moment of $6 \mu_B$. We should also note here that ferromagnetism is stabilized by the inter-sublattice interactions between the Mn(Cr) and Co atoms and between Co atoms belonging to different sublattices as shown by first-principles calculations.^{32,33}

Before closing this section we should discuss also the role of the sp -elements in half-metallic Heusler alloys. While the sp -elements are not responsible for the appearance of the minority gap, they are very important for the physical properties of the Heusler alloys and their structural stability. sp atoms provide one s and three p bands per spin which lay very low in energy and accommodate d -electrons of the transition metal atoms. Thus the effective d -charge, which is accommodated by transition-metal atomic d -hybrids, is reduced stabilizing

the half-metallicity. These s- and p-states of the sp atom strongly hybridize with the transition metal d-states and the charge in these bands is delocalized and locally the sp atoms even lose charge in favor of the transition metal atoms.

III. DEFECTS IN FULL-HEUSLERS CONTAINING Co AND Mn

In this section we discuss results on the defects in the case of Co_2MnZ alloys where Z is Al and Si.^{23,24} To simulate the doping by electrons we substitute Fe for Mn while to simulate the doping of the alloys with holes we substitute Cr for Mn and we have considered the cases of moderate doping substituting 5% and 10% of the Mn atoms and we present our results in figure 2 for the Co_2MnSi and Co_2MnAl compounds. As discussed in the previous section the gap is created between states located exclusively at the Co sites. The states low in energy (around -6 eV below the Fermi level) originate from the low-lying p-states of the sp atoms and the ones at around -9 eV below the Fermi level are the s-states of the sp-atom. The majority-spin occupied states form a common Mn-Co band while the occupied minority states are mainly located at the Co sites and the minority unoccupied states at the Mn sites. The extra electron in the the Co_2MnSi alloy occupies majority states leading to an increase of the exchange splitting between the occupied majority and the unoccupied minority states and thus to larger gap-width for the Si-based compound. In the case of the Al-based alloy the bonding and antibonding minority d-hybrids almost overlap and the gap is substituted by a region of very small minority density of states (DOS); we will call it a pseudogap. In both cases the Fermi level falls within the gap (Co_2MnSi) or the pseudogap (Co_2MnAl) and an almost perfect spin-polarization at the Fermi level is preserved.

Doping the perfect ordered alloys with either Fe or Cr smoothens the valleys and peaks along the energy axis. This is a clear sign of the chemical disorder; Fe and Cr induce peaks at slightly different places than the Mn atoms resulting to this smoothing and as the doping increases this phenomenon becomes more intense. The important detail is what happens around the Fermi level and in what extent is the gap in the minority band affected by the doping. So now we will concentrate only at the enlarged regions around the Fermi level. The dashed lines represent the Cr-doping while the dotted lines are the Fe-doped alloys. Cr-doping in Co_2MnSi has only a marginal effect to the gap. Its width is narrower with respect to the perfect compounds but overall the compounds retain their half-metallicity. For Co_2MnAl the situation is reversed with respect to the Co_2MnSi compound and Cr-doping has significant effects on the pseudogap. Its width is larger with respect to the perfect compound and becomes slightly narrower as the degree of doping increases.

In the case of Fe-doping the situation is more com-

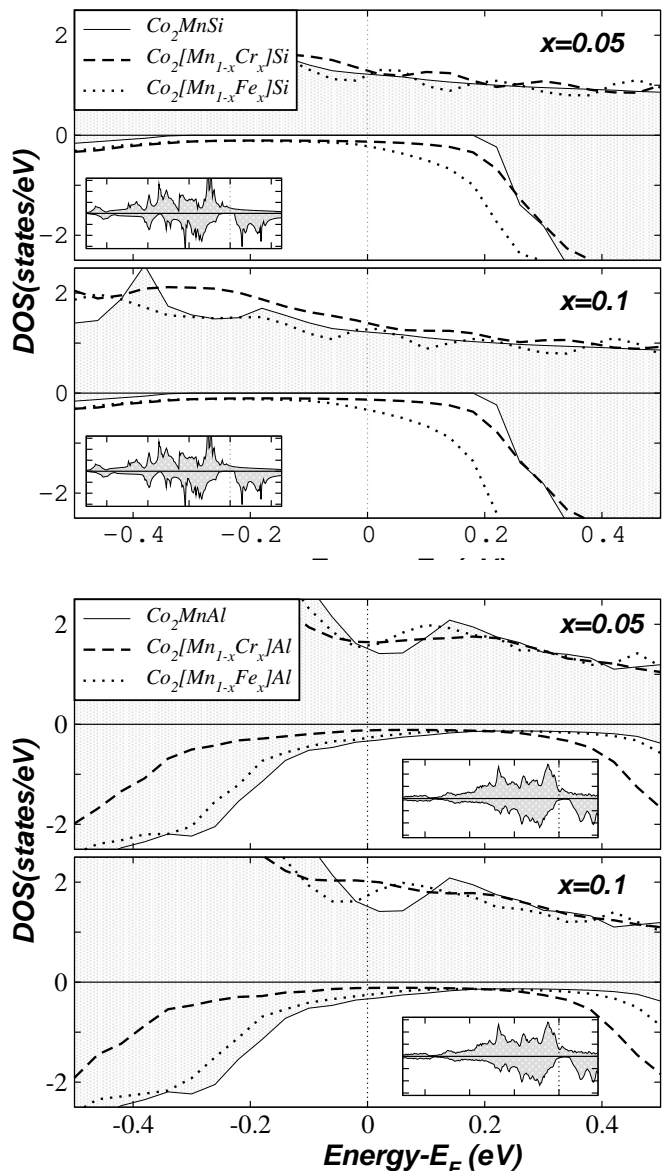


FIG. 2: Spin-resolved density of states (DOS) for the case of $\text{Co}_2[\text{Mn}_{1-x}\text{Cr}_x]\text{Si}$ and $\text{Co}_2[\text{Mn}_{1-x}\text{Fe}_x]\text{Si}$ in the upper panel, and $\text{Co}_2[\text{Mn}_{1-x}\text{Cr}_x]\text{Al}$ and $\text{Co}_2[\text{Mn}_{1-x}\text{Fe}_x]\text{Al}$ in the lower panel for two values of the doping concentration x . DOS's are compared to the one of the undoped Co_2MnSi and Co_2MnAl alloys. The zero of the energy axis corresponds to the Fermi energy. Positive values of the DOS correspond to the majority-spin (spin-up) electrons and negative values to the minority-spin (spin-down) electrons. In the insets we present the DOS for a wider energy range.

plex. Adding electrons to the system means that, in order to retain the perfect half-metallicity, these electrons should occupy high-energy lying antibonding majority states. This is energetically not very favorable in the case of Co_2MnSi and for these moderate degrees of doping a new shoulder appears in the unoccupied states which is close to the right-edge of the gap; a sign of a large change in the competition between the exchange

splitting of the Mn majority and minority states and of the Coulomb repulsion. In the case of the 20% Fe doping in Co_2MnSi (not shown here) this new peak crosses the Fermi level and the Fermi level is no more exactly in the gap but slightly above it. Further substitution should lead to the complete destruction of the half-metallicity.³⁴ Recent ab-initio calculations including the on-site Coulomb repulsion (the so-called Hubbard U) have predicted that Co_2FeSi is in reality half-metallic reaching a total spin magnetic moment of $6 \mu_B$ which is the largest known spin moment for a half-metal.^{31,35} Fe-doping on the other hand in Co_2MnAl almost does not change the DOS around the Fermi level. The extra-electrons occupy high-energy lying antibonding majority states but, since Co_2MnAl has one valence electron less than Co_2MnSi , half-metallicity remains energetically favorable and no important changes occur upon Fe-doping and further substitution of Fe for Mn should retain the half-metallicity even for the Co_2FeAl compound although LDA-based ab-initio calculations predict that the limiting case of Co_2FeAl is almost half-metallic.³⁴

IV. DEFECTS DRIVEN HALF-METALLIC FERRIMAGNETISM

In the previous section we have examined the case of defects in half-metallic ferromagnets. Half-metallic ferrimagnetism (HMF_i) on the other hand is highly desirable since such compounds would yield lower total spin moments than the corresponding ferromagnets. Well-known HMF_i are the perfect Heusler compounds FeMnSb and Mn_2VAI .³⁶ We will present in the first part of this section another route to half-metallic ferrimagnetism based on antisites created by the migration of Cr(Mn) atoms at Co sites in the case of Co_2CrAl , Co_2CrSi , Co_2MnAl and Co_2MnSi alloys. The ideal case for applications would be a fully-compensated ferrimagnet, also known as half-metallic antiferromagnet (HMA),³⁷ since such a compound would not give rise to stray flux and thus would lead to smaller energy consumption in devices. In the second part of this section we present a way to achieve HMA based on Co defects in half-metallic ferrimagnets like Mn_2VAI .

We will start our discussion from the Cr-based alloys and using Co_2CrAl and Co_2CrSi as parent compounds we create a surplus of Cr atoms which sit at the perfect Co sites. In figure 3 we present the total density of states (DOS) for the $[\text{Co}_{1-x}\text{Cr}_x]_2\text{CrAl}$ and $[\text{Co}_{1-x}\text{Cr}_x]_2\text{CrSi}$ alloys for concentrations $x=0$ and 0.1, and in table I we have gathered the spin moments for the two compounds under study. We will start our discussion from the DOS. The perfect compounds show a gap in the minority-spin band and the Fermi level falls within this gap and thus the compounds are half-metals. When the sp atom is Si instead of Al the gap is larger due to the extra electron which occupies majority states of the transition metal atoms²⁹ and increases the exchange splitting between the

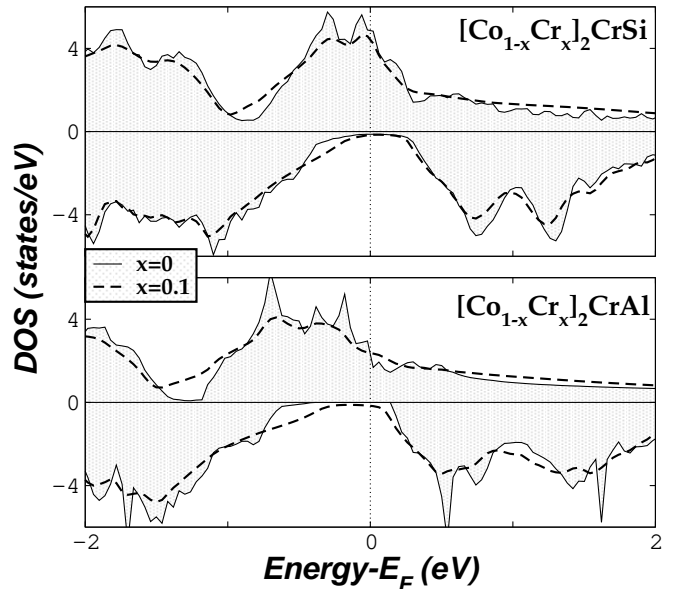


FIG. 3: Total density of states (DOS) as a function of the concentration x for the $[\text{Co}_{1-x}\text{Cr}_x]_2\text{CrAl}$ (upper panel) and $[\text{Co}_{1-x}\text{Cr}_x]_2\text{CrSi}$ (lower panel) compounds.

TABLE I: Atom-resolved spin magnetic moments for the $[\text{Co}_{1-x}\text{Cr}_x]_2\text{CrAl}$, $[\text{Co}_{1-x}\text{Cr}_x]_2\text{CrSi}$, $[\text{Co}_{1-x}\text{Mn}_x]_2\text{MnAl}$ and $[\text{Co}_{1-x}\text{Mn}_x]_2\text{MnSi}$ compounds (moments have been scaled to one atom). The two last columns are the total spin moment (Total) in the unit cell calculated as $2 \times [(1-x) * m^{\text{Co}} + x * m^{\text{Cr or Mn(imp)}}] + m^{\text{Cr(Mn)}} + m^{\text{Al or Si}}$ and the ideal total spin moment predicted by the Slater-Pauling rule for half-metals (see section II). With IMP we denote the Cr(Mn) atoms sitting at perfect Co sites.

Compound	Co	IMP	Cr/Mn	Al/Si	Total	Ideal
Co_2CrAl	0.73	-	1.63	-0.09	3.00	3.00
$[\text{Co}_{0.95}\text{Cr}_{0.05}]_2\text{CrAl}$	0.71	-1.82	1.62	-0.09	2.70	2.70
$[\text{Co}_{0.9}\text{Cr}_{0.1}]_2\text{CrAl}$	0.69	-1.85	1.61	-0.08	2.40	2.40
Co_2CrSi	0.95	-	2.17	-0.06	4.00	4.00
$[\text{Co}_{0.95}\text{Cr}_{0.05}]_2\text{CrSi}$	0.93	-1.26	2.12	-0.06	3.70	3.70
$[\text{Co}_{0.9}\text{Cr}_{0.1}]_2\text{CrSi}$	0.91	-1.26	2.07	-0.05	3.40	3.40
Co_2MnAl	0.68	-	2.82	-0.14	4.04	4.00
$[\text{Co}_{0.95}\text{Mn}_{0.05}]_2\text{MnAl}$	0.73	-2.59	2.82	-0.13	3.81	3.80
$[\text{Co}_{0.9}\text{Mn}_{0.1}]_2\text{MnAl}$	0.78	-2.49	2.83	-0.12	3.61	3.60
Co_2MnSi	0.98	-	3.13	-0.09	5.00	5.00
$[\text{Co}_{0.95}\text{Mn}_{0.05}]_2\text{MnSi}$	0.99	-0.95	3.09	-0.08	4.80	4.80
$[\text{Co}_{0.9}\text{Mn}_{0.1}]_2\text{MnSi}$	0.99	-0.84	3.06	-0.07	4.60	4.60

majority occupied and the minority unoccupied states. This electron increases the Cr spin moment by $\sim 0.5 \mu_B$ and the moment of each Co atom by $\sim 0.25 \mu_B$ about. The Cr and Co majority states form a common band and the weight at the Fermi level is mainly of Cr character. The minority occupied states are mainly of Co character. When we substitute Cr for Co, the effect on the atomic DOS of the Co and Cr atoms at the perfect sites is marginal. The DOS of the impurity Cr atoms has a completely different form from the Cr atoms at the per-

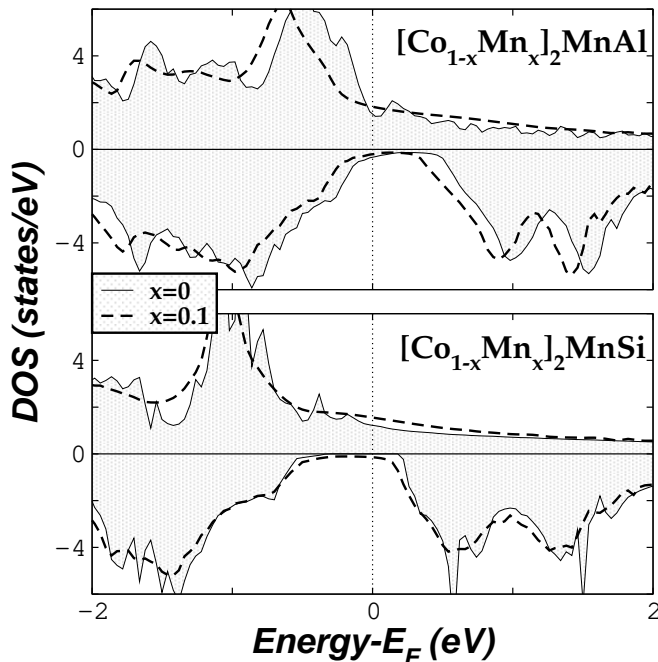


FIG. 4: Total density of states (DOS) around the gap region for the $[\text{Co}_{1-x}\text{Mn}_x]_2\text{MnAl}$ and $[\text{Co}_{1-x}\text{Mn}_x]_2\text{MnSi}$ alloys as a function of the concentration x : we denote $x = 0$ with the solid line and $x = 0.1$ with a dashed thick line.

fect sites due to the different symmetry of the site where they sit. But although Cr impurity atoms at the antisites induce minority states within the gap, there is still a tiny gap and the Fermi level falls within this gap keeping the half-metallic character of the parent compounds.

The discussion above on the conservation of the half-metallicity is confirmed when we compare the calculated total moments in table I with the values predicted by the Slater Pauling rule for the ideal half-metals. Since Cr is lighter than Co, substitution of Cr for Co decreases the total number of valence electrons and the total spin moment should also decrease. This is achieved due to the antiferromagnetic coupling between the Cr impurity atoms and the Co and Cr ones at the ideal sites, which would have an important negative contribution to the total moment as confirmed by the results in table I. Thus the Cr-doped alloys are half-metallic ferrimagnets and their total spin moment is considerable smaller than the perfect half-metallic ferromagnetic parent compounds; in the case of $[\text{Co}_{0.8}\text{Cr}_{0.2}]_2\text{CrAl}$ it decreases down to $1.8 \mu_B$ from the $3 \mu_B$ of the perfect Co_2CrAl alloy. Here we have to mention that if also Co atoms migrate to Cr sites (case of atomic swaps) the half-metallicity is lost, as it was shown by Miura et al.³⁸, due to the energy position of the Co states which have migrated at Cr sites.

Similar phenomena to the discussion above occur in the $[\text{Co}_{1-x}\text{Mn}_x]_2\text{MnZ}$ compounds varying the sp atom, Z, which is one of Al or Si. We have taken into account five different values for the concentration x ; $x = 0, 0.025,$

$0.05, 0.1, 0.2$. In figure 4 we have drawn the total density of states (DOS) for both families of compounds under study and for two different values of the concentration x : the perfect compounds ($x=0$) and for one case with defects, $x=0.1$. As mentioned above and in agreement with previous previous electronic structure calculations on these compounds Co_2MnSi compounds present a real gap and Co_2MnAl a pseudogap.^{23,29,39,40} When we create a surplus of Mn atoms which migrate at sites occupied by Co atoms in the perfect alloys, the gap persists and both compounds retain their half-metallic character as occurs also for the Cr-based alloys presented above. Especially for Co_2MnSi , the creation of Mn antisites does not alter the width of the gap and the half-metallicity is extremely robust in these alloys with respect to the creation of Mn antisites. The atomic spin moments show behavior similar to the Cr alloys as can be seen in table I and the spin moments of the Mn impurity atoms are antiferromagnetically coupled to the spin moments of the Co and Mn atoms at the perfect sites resulting to the desired half-metallic ferrimagnetism.

The ideal case of fully-compensated half-metallic ferrimagnet or half-metallic antiferromagnetic (HMA) can be achieved by doping with Co the Mn_2VAl and Mn_2VSi alloys which are well known to be HMF_i. The importance of this route stems from the existence of Mn_2VAl in the Heusler $L2_1$ phase as shown by several groups.^{41,42,43} Each Mn atom has a spin moment of around $-1.5 \mu_B$ and V atom a moment of about $0.9 \mu_B$.^{41,42,43}

All theoretical studies on Mn_2VAl agree on the half-metallic character with a gap at the spin-up band instead of the spin-down band as for the other half-metallic Heusler alloys.^{29,44,45,46} Prior to the presentation of our results we have to note that due to the Slater-Pauling rule, these compounds with less than 24 valence electrons have negative total spin moments and the gap is located at the spin-up band. Moreover the spin-up electrons correspond to the minority-spin electrons and the spin-down electrons to the majority electrons contrary to the other Heusler alloys.²⁹ We have substituted Co for Mn in $\text{Mn}_2\text{V}(\text{Al or Si})$ in a random way and in figure 5 we present the total and atom-resolved density of states (DOS) in $[\text{Mn}_{1-x}\text{Co}_x]_2\text{VAl}$ (solid line) and $[\text{Mn}_{1-x}\text{Co}_x]_2\text{VSi}$ (dashed line) alloys for $x=0.1$. The perfect compounds show a region of low spin-up DOS (we will call it a “pseudogap”) instead of a real gap. Upon doping the pseudogap at the spin-up band persists and the quaternary alloys keep the half-metallic character of the perfect Mn_2VAl and Mn_2VSi compounds. Co atoms are strongly polarized by the Mn atoms since they occupy the same sublattice and they form Co-Mn hybrids which afterwards interact with the V and Al or Si states.²⁹ The spin-up Co states form a common band with the Mn ones and the spin-up DOS for both atoms has similar shape. Mn atoms have less weight in the spin-down band since they accommodate less charge than the heavier Co atoms.

In table II we have gathered the total and atom-

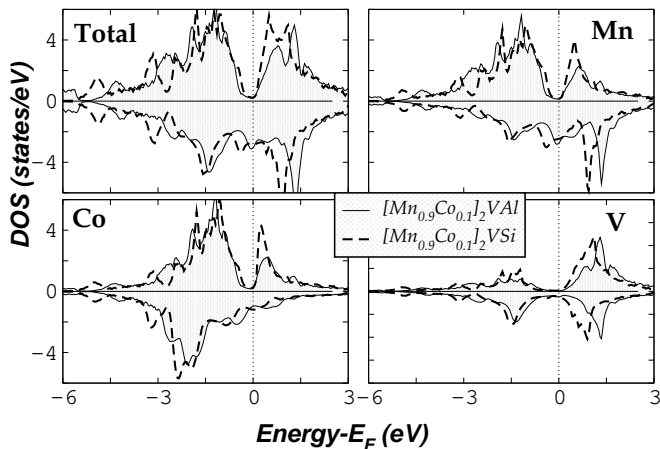


FIG. 5: Total and atom-resolved DOS for the $[\text{Mn}_{0.9}\text{Co}_{0.1}]_2\text{VAI}$ and $[\text{Mn}_{0.9}\text{Co}_{0.1}]_2\text{VSi}$ compounds. Note that the atomic DOS's have been scaled to one atom.

resolved spin moments for all the Co-doped compounds as a function of the concentration. We have gone up to a concentration which corresponds to 24 valence electrons in the unit cell, thus up to $x=0.5$ for the $[\text{Mn}_{1-x}\text{Co}_x]_2\text{VAI}$ and $x=0.25$ for the $[\text{Mn}_{1-x}\text{Co}_x]_2\text{VSi}$ alloys. In the last column we have included the total spin moment predicted by the Slater-Pauling rule for the perfect half-metals. A comparison between the calculated and ideal total spin moments reveals that all the compounds under study are half-metals with very small deviations due to the existence of a pseudogap instead of a real gap. Exactly for 24 valence electrons the total spin moment vanishes as we will discuss in the next paragraph. Co atoms have a spin moment parallel to the V one and antiparallel to the Mn moment, and thus the compounds retain their ferrimagnetic character. As we increase the concentration of the Co atoms in the alloys, each Co has more Co atoms as neighbors, it hybridizes stronger with them and its spin moment increases while the spin moment of the Mn atom decreases (these changes are not too drastic). The sp atoms have a spin moment antiparallel to the Mn atoms as already discussed in reference 47.

The most interesting point in this substitution procedure is revealed when we increase the Co concentration to a value corresponding to 24 valence electrons in the unit cell, thus the $[\text{Mn}_{0.5}\text{Co}_{0.5}]_2\text{VAI}$ and $[\text{Mn}_{0.75}\text{Co}_{0.25}]_2\text{VSi}$ alloys. The Slater-Pauling rule predicts for these compounds a zero total spin moment in the unit cell and the electrons population is equally divided between the two spin-bands. Our first-principles calculations reveal that this is actually the case. The interest arises from the fact that although the total moment is zero, these two compounds are made up from strongly magnetic components. Mn atoms have a mean spin moment of $\sim -1.4 \mu_B$ in $[\text{Mn}_{0.5}\text{Co}_{0.5}]_2\text{VAI}$ and $\sim -0.9 \mu_B$ in $[\text{Mn}_{0.75}\text{Co}_{0.25}]_2\text{VSi}$. Co and V have spin moments antiferromagnetically coupled to the Mn ones which for $[\text{Mn}_{0.5}\text{Co}_{0.5}]_2\text{VAI}$ are ~ 0.6

TABLE II: Atom-resolved spin magnetic moments for the $[\text{Mn}_{1-x}\text{Co}_x]_2\text{VAI}$ and $[\text{Mn}_{1-x}\text{Co}_x]_2\text{VSi}$ compounds (moments have been scaled to one atom). The two last columns are the total spin moment (Total) in the unit cell calculated as $2 \times [(1-x) * m^{\text{Mn}} + x * m^{\text{Co}}] + m^{\text{V}} + m^{\text{Al or Si}}$ and the ideal total spin moment predicted by the Slater-Pauling rule for half-metals. The lattice constants have been chosen 0.605 nm for Mn_2VAI and 0.6175 for Mn_2VSi for which both systems are half-metals (see reference 47) and have been kept constant upon Co doping.

Compound	Mn	Co	V	Al	Total	Ideal
Mn_2VAI	-1.57	-	1.08	0.06	-2.00	-2.0
$[\text{Mn}_{0.9}\text{Co}_{0.1}]_2\text{VAI}$	-1.56	0.340	1.07	0.07	-1.60	-1.6
$[\text{Mn}_{0.7}\text{Co}_{0.3}]_2\text{VAI}$	-1.48	0.46	0.95	0.05	-0.80	-0.8
$[\text{Mn}_{0.5}\text{Co}_{0.5}]_2\text{VAI}$	-1.39	0.59	0.78	0.02	~ 0	0
Compound	Mn	Co	V	Si	Total	Ideal
Mn_2VSi	-0.96	-	0.86	0.06	-1.00	-1.0
$[\text{Mn}_{0.9}\text{Co}_{0.1}]_2\text{VSi}$	-0.93	0.82	0.85	0.05	-0.60	-0.6
$[\text{Mn}_{0.75}\text{Co}_{0.25}]_2\text{VSi}$	-0.90	0.94	0.84	0.04	~ 0	0

and $\sim 0.8 \mu_B$, respectively, and for $[\text{Mn}_{0.75}\text{Co}_{0.25}]_2\text{VSi}$ ~ 0.9 and $\sim 0.8 \mu_B$. Thus these two compounds are half-metallic fully-compensated ferrimagnets or as they are best known in literature half-metallic antiferromagnets.

V. SUMMARY AND CONCLUSIONS

In this chapter we have reviewed our results on the defects in half-metallic full-Heusler alloys. Firstly we have presented a short overview of the electronic and magnetic properties of the half-metallic full-Heusler alloys and have discussed in detail the Slater-Pauling behavior of these alloys (the total spin moment scales linearly with the total number of valence electrons as a result of the half-metallicity). We have also studied the effect of doping on the magnetic properties of the $\text{Co}_2\text{MnAl}(\text{Si})$ full-Heusler alloys. Doping simulated by the substitution of Cr and Fe for Mn overall keeps the half-metallicity and has little effect on the half-metallic properties of Co_2MnSi and Co_2MnAl compounds.

Afterwards, we have studied the effect of defects-driven appearance of half-metallic ferrimagnetism in the case of the $\text{Co}_2\text{Cr}(\text{Mn})\text{Al}(\text{Si})$ Heusler alloys. More precisely, based on first-principles calculations we have shown that when we create Cr(Mn) antisites at the Co sites, these impurity Cr(Mn) atoms couple antiferromagnetically with the Co and the Cr(Mn) atoms at the perfect sites while keeping the half-metallic character of the parent compounds. The ideal case of half-metallic fully-compensated ferrimagnets (also known as half-metallic antiferromagnets) can be achieved by doping of the half-metallic ferrimagnets Mn_2VAI and Mn_2VSi . Co substitution for Mn keeps the half-metallic character of the parent compounds and when the total number of valence electrons reaches the 24, the total spin moment vanishes as predicted by the Slater-Pauling rule. Defects are a

promising alternative way to create robust half-metallic ferrimagnets, which are crucial for magnetoelectronic ap-

plications.

-
- * Electronic address: kozdogan@gyte.edu.tr
 † Electronic address: e.sasioglu@fz-juelich.de
 ‡ Electronic address: galanakis@upatras.gr
- ¹ R. A. de Groot, F. M. Mueller, P. G. van Engen, and K. H. J. Buschow, *Phys. Rev. Lett.* **50**, 2024 (1983).
 - ² I. Žutić, J. Fabian, and A. Das Sarma, *Rev. Mod. Phys.* **76**, 323 (2004)
 - ³ P. J. Webster and K. R. A. Ziebeck in *Alloys and Compounds of d-Elements with Main Group Elements. Part 2.*, Landolt-Börnstein, New Series, Group III, vol 19c, ed. by H. R. J. Wijn, (Springer, Berlin 1988) pp 75–184.
 - ⁴ K. R. A. Ziebeck and K. -U. Neumann in *Magnetic Properties of Metals*, Landolt-Börnstein, New Series, Group III, vol 32/c, ed. by H. R. J. Wijn, (Springer, Berlin 2001) pp 64–414.
 - ⁵ R. J. Soulen Jr., J. M. Byers, M. S. Osofsky, B. Nadgorny, T. Ambrose, S. F. Cheng, P. R. Broussard, C. T. Tanaka, J. Nowak, J. S. Moodera, A. Barry, and J. M. D. Coey, *Science* **282**, 85 (1998).
 - ⁶ K. A. Kilian and R. H. Victora, *J. Appl. Phys.* **87**, 7064 (2000).
 - ⁷ C. T. Tanaka, J. Nowak, and J. S. Moodera, *J. Appl. Phys.* **86**, 6239 (1999).
 - ⁸ J. A. Caballero, Y. D. Park, J. R. Childress, J. Bass, W. -C. Chiang, A. C. Reilly, W. P. Pratt Jr., and F. Petroff, *J. Vac. Sci. Technol. A* **16**, 1801 (1998); C. Hordequin, J. P. Nozières, and J. Pierre. *J. Magn. Magn. Mater.* **183**, 225 (1998).
 - ⁹ A. Bergmann, J. Grabis, B. P. Toperverg, V. Leiner, M. Wolff, H. Zabel, and K. Westerholt, *Phys. Rev. B* **72**, 214403 (2005); J. Grabis, A. Bergmann, A. Nefedov, K. Westerholt, and H. Zabel, *Phys. Rev. B* **72**, 024437 (2005); *idem*, *Phys. Rev. B* **72**, 024438 (2005).
 - ¹⁰ S. Kämmerer, A. Thomas, A. Hütten, and G. Reiss, *Appl. Phys. Lett.* **85**, 79 (2004).
 - ¹¹ J. Schmalhorst, S. Kämmerer, M. Sacher, G. Reiss, A. Hütten, and A. Scholl, *Phys. Rev. B* **70**, 024426 (2004).
 - ¹² Y. Sakuraba, M. Hattori, M. Oogane, Y. Ando, H. Kato, A. Sakuma, T. Miyazaki, and H. Kubota, *Appl. Phys. Lett.* **88**, 192508 (2006); Y. Sakuraba, J. Nakata, M. Oogane, Y. Ando, H. Kato, A. Sakuma, T. Miyazaki, and H. Kubota, *Appl. Phys. Lett.* **88**, 022503 (2006); Y. Sakuraba, T. Miyakoshi, M. Oogane, Y. Ando, A. Sakuma, T. Miyazaki, and H. Kubota, *Appl. Phys. Lett.* **89**, 052508 (2006); Y. Sakuraba, J. Nakata, M. Oogane, H. Kubota, Y. Ando, A. Sakuma, and T. Miyazaki, *Jpn. J. Appl. Phys.* **44**, L1100 (2005).
 - ¹³ X. Y. Dong, C. Adelman, J. Q. Xie, C. J. Palmström, X. Lou, J. Strand, P. A. Crowell, J.-P. Barnes, and A. K. Petford-Long, *Appl. Phys. Lett.* **86**, 102107 (2005).
 - ¹⁴ N. Papanikolaou, R. Zeller, and P. H. Dederichs, *J. Phys.: Condens. Matter* **14**, 2799 (2002).
 - ¹⁵ I. Galanakis, Ph. Mavropoulos, and P. H. Dederichs, *J. Phys. D: Appl. Phys.* **39**, 765 (2006).
 - ¹⁶ Half-metallic alloys: fundamentals and applications, Eds.: I. Galanakis and P. H. Dederichs, *Lecture notes in Physics* vol. 676 (Berlin Heidelberg: Springer 2005).
 - ¹⁷ "Electronic and Magnetic Properties of the Normal and Quaternary Full-Heusler Alloys: The Quest for New Half-Metallic Ferromagnets", I. Galanakis, in "New Developments in Ferromagnetism Research", V.N. Murray (ed.), (Nova Publishers, New York 2005), pp 79-97.
 - ¹⁸ K. Koepnik and H. Eschrig, *Phys. Rev. B* **59**, 3174 (1999).
 - ¹⁹ K. Koepnik, B. Velicky, R. Hayn, and H. Eschrig, *Phys. Rev. B* **58**, 6944 (1998).
 - ²⁰ P. Hohenberg and W. Kohn, *Phys. Rev.* **136**, B864 (1964).
 - ²¹ W. Kohn and L. J. Sham, *Phys. Rev.* **140**, A1133 (1965).
 - ²² J. P. Perdew and Y. Wang, *Phys. Rev. B* **45**, 13244 (1992).
 - ²³ I. Galanakis, K. Özdoğan, B. Aktaş, and E. Şaşıoğlu, *Appl. Phys. Lett.* **89**, 042502 (2006).
 - ²⁴ K. Özdoğan, E. Şaşıoğlu, B. Aktaş, and I. Galanakis, *Phys. Rev. B* **74**, 172412 (2006).
 - ²⁵ S. Picozzi and A. J. Freeman, *J. Phys.: Condens. Matter* **19**, 315215 (2007).
 - ²⁶ K. Özdoğan, I. Galanakis, E. Şaşıoğlu, and B. Aktaş, *Phys. Stat. Sol. (RRL)* **1**, 95 (2007).
 - ²⁷ K. Özdoğan, I. Galanakis, E. Şaşıoğlu, and B. Aktaş, *Sol. St. Commun.* **142**, 492 (2007).
 - ²⁸ I. Galanakis, K. Özdoğan, E. Şaşıoğlu, and B. Aktaş, *Phys. Rev. B* **75**, 092407 (2007).
 - ²⁹ I. Galanakis, P. H. Dederichs, and N. Papanikolaou, *Phys. Rev. B* **66**, 174429 (2002).
 - ³⁰ I. Galanakis, P. H. Dederichs, and N. Papanikolaou, *Phys. Rev. B* **66**, 134428 (2002).
 - ³¹ H. M. Kandpal, G. H. Fecher, C. Felser, and G. Schönhense, *Phys. Rev. B* **73**, 094422 (2006).
 - ³² E. Şaşıoğlu, L. M. Sandratskii, P. Bruno, and I. Galanakis, *Phys. Rev. B* **72**, 184415 (2005).
 - ³³ Y. Kurtulus, R. Dronskowski, G. D. Samolyuk, and V. P. Antropov, *Phys. Rev. B* **71**, 014425 (2005).
 - ³⁴ I. Galanakis, *J. Phys.: Condens. Matter* **16**, 3089 (2004).
 - ³⁵ S. Wurmehl, G. H. Fecher, H. C. Kandpal, V. Ksenofontov, C. Felser, and H. -J. Lin, *Appl. Phys. Lett.* **88**, 032503.
 - ³⁶ R. A. de Groot, A. M. van der Kraan, and K. H. J. Buschow, *J. Magn. Magn. Mater.* **61**, 330 (1986).
 - ³⁷ H. van Leuken and R. A. de Groot, *Phys. Rev. Lett.* **74**, 1171 (1995).
 - ³⁸ Y. Miura, K. Nagao, and M. Shirai, *Phys. Rev. B* **69**, 144413 (2004).
 - ³⁹ M. Sargolzaei, M. Richter, K. Koepnik, I. Opahle, H. Eschrig, and I. Chaplygin, *Phys. Rev. B* **74**, 224410 (2006).
 - ⁴⁰ K. Özdoğan, B. Aktaş, I. Galanakis, and E. Şaşıoğlu, *J. Appl. Phys.* **101**, 073910 (2007).
 - ⁴¹ Y. Yoshida, M. Kawakami, and T. Nakamichi, *J. Phys. Soc. Jpn.* **50**, 2203 (1981).
 - ⁴² H. Itoh, T. Nakamichi, Y. Yamaguchi, and N. Kazama, *Trans. Jpn. Inst. Met.* **24**, 265 (1983).
 - ⁴³ C. Jiang, M. Venkatesan, and J. M. D. Coey, *Sol. St. Commun.* **118**, 513 (2001).
 - ⁴⁴ E. Şaşıoğlu, L. M. Sandratskii, and P. Bruno, *J. Phys.: Condens. Matter* **17**, 995 (2005).
 - ⁴⁵ S. Ishida, S. Asano, and J. Ishida, *J. Phys. Soc. Jpn.* **53**, 2718 (1984).

⁴⁶ R. Weht and W. E. Pickett, Phys. Rev. B **60**, 13006 (1999).

⁴⁷ K. Özdoğan, I. Galanakis, E. Şaşıoğlu, and B. Aktaş, J.

Phys.: Condens. Matter **18**, 2905 (2006).